Pure Appl. Chem., Vol. 72, Nos. 1–2, pp. 317–325, 2000.

Core/shell-structured bimetallic nanocluster catalysts for visible-light-induced electron transfer*

Naoki Toshima

Department of Materials Science and Engineering, Science University of Tokyo in Yamaguchi, Onoda-shi, Yamaguchi 756-0884, Japan

Abstract: It has been found that the bimetallic nanoclusters often have so-called core/shell structure if they are prepared by alcohol-reduction of two kinds of noble metal ions in the presence of a water-soluble polymer like poly(N-vinyl-2-pyrolidone)(PVP), and that the core/shell structured bimetallic nanoclusters have much higher catalytic activity than the corresponding monometallic nanoclusters. Here, several kinds of monometallic and bimetallic nanoclusters are synthesized by the similar method, and the catalyses are measured. Thus, the colloidal dispersions of Au, Pt, Pd, Rh, and Ru monometallic, and Au/Pt, Au/Pd, Au/Rh, and Pt/Ru bimetallic nanoclusters were synthesized and applied as the catalysts for visible-light-induced hydrogen generation. The core/shell structures are analyzed mainly by UV–vis spectra. The rate of electron transfer from the methyl viologen cation radical to the metal nanoclusters is proportional to the hydrogen generation rate at the steady state. All the electrons accepted by the metal nanoclusters are used for the hydrogen generation. Both electron transfer and hydrogen generation rates increase when the bimetallic nanoclusters are used in place of the corresponding monometallic nanoclusters. The most active catalysts were Au/Rh and Pt/Ru bimetallic nanoclusters.

INTRODUCTION

Metal nanoclusters are known as one of the most important advanced materials [1]. The most remarkable features of metal nanoclusters are their specific chemical and physical properties. Among the chemical properties of metal nanoclusters, catalysis is of great interest and is the best investigated.

Bimetallic nanoclusters, composed of two different metal elements, are of greater interest than monometallic ones, from both the scientific and technological views, for the improvement of catalytic properties of metal particles. In fact, we have found that the bimetallic nanoclusters often have so-called core/shell structure if they are prepared by alcohol-reduction of two kinds of noble metal ions in the presence of a water-soluble polymer like poly(N-vinyl-2-pyrolidone)(PVP), and that the core/shell-structured bimetallic nanoclusters have much higher catalytic activity than the corresponding monometallic nanoclusters [2]. The core/shell structure was suggested by UV–vis spectra, XPS spectra, catalytic properties, etc., and finally analyzed by an EXAFS technique [3].

On the other hand, noble metal nanoclusters can work as a catalyst for visible light-induced hydrogen generation from water in the system like EDTA/tris(bipyridine)ruthenium(II)/methyl viologen/colloidal metal catalyst as shown in Fig. 1 [4]. The Au/Pt bimetallic nanoclusters, especially those having an Au-core/Pt-shell structure were found to work as a more active catalyst for the hydrogen

Pure Appl. Chem.* **72, 1–331 (2000). An issue of reviews and research papers based on lectures presented at the 1st IUPAC Workshop on Advanced Materials (WAM1), Hong Kong, July 1999, on the theme of nanostructured systems.

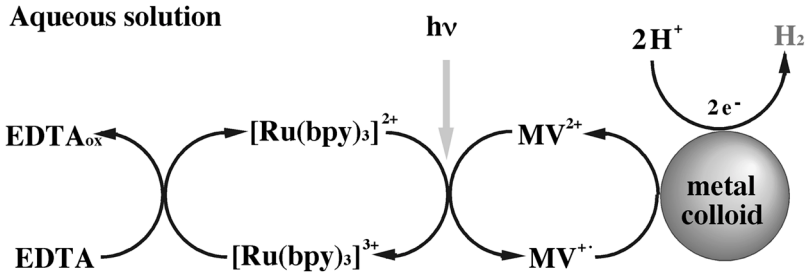

Fig. 1 Schematic illustration of visible-light-induced hydrogen generation in the system of EDTA/ tris(bipyridine)ruthenium(II)/methyl viologen/colloidal metal catalyst.

generation in the above system than the conventional Pt nanocluster catalyst [5]. Here, we would like to present the results of the syntheses and catalyses of several kinds of monometallic and bimetallic nanoclusters, and to discuss the results on the basis of electron transfer rates from methyl viologen cation radical to metal nanoclusters.

BIMETALLIC NANOCLUSTERS

Colloidal dispersions of bimetallic nanoclusters have not been well-examined until recently. Colloidal dispersions of Ag/Au bimetallic nanoclusters were prepared by γ-irradiation for the study of electrochemical reactions [6]. Trimetallic nanoclusters were also prepared by the same method and applied to investigation of optical properties [7]. Ag/Pt and Ag/Pd bimetallic nanoclusters were obtained by reduction of the corresponding double complexes [8]. Bönnemann et al. used hydrotriorganoborates as a reductant to get Pt/Rh bimetallic nanoclusters, and applied to catalysts for hydrogenation of crotonic acid [9]. Cu/Pd bimetallic nanoclusters were prepared by thermal decomposition of the mixtures of the corresponding metal acetates [10], while the exact Cu/Pd bimetallic nanoclusters with 0-valent Cu were prepared with a modified polyol process [11].

When alcohol-reduction in the presence of PVP is applied to the mixtures of two kinds of noble metal ions, not the mixtures of two kinds of monometallic nanoclusters, but bimetallic nanoclusters, each particle of which is composed of two kinds of elements, can be obtained in a series of combinations of two kinds of noble metals, such as Au/Pt, Au/Pd, Pd/Pt, and Pt/Rh [2,3]. The structures of these bimetallic nanoclusters were carefully analyzed by the combination of various analytical methods, especially by an EXAFS technique. Interestingly, the so-called core/shell structure has been found to be common for the four couples examined.

For example, Pd/Pt bimetallic nanoclusters have an average diameter of ca. 1.4 nm corresponding to 55 atoms with an fcc structure. When the charged atomic ratio of Pd/Pt is 4:1, the exact core/shell-structured model, shown in Fig. 2 (upper), can be proposed. In this model, 13 Pt atoms form a core, and 42 Pd atoms surround the core to form a shell. When the Pd/Pt ratio is 1:1, then a modified core/shell structure model, shown in Fig. 2 (lower), can be proposed on the ratio of EXAFS analysis.

The Pd/Pt bimetallic nanoclusters with various Pd/Pt ratios are applied to the catalysis for selective partial hydrogenation of 1,3-cyclooctadiene to cyclooctene under mild conditions. Interestingly, the bimetallic nanoclusters at Pd/Pt = 4 have the highest catalytic activity for the reaction. It is known that Pd monometallic nanoclusters are a good catalyst for the above partial hydrogenation, while Pt monometallic nanoclusters a poor catalyst. Nevertheless, the Pd/Pt bimetallic nanoclusters are better catalysts than Pd monometallic nanoclusters. This means that the surface Pd atoms neighbored by Pt core are more active than the surface Pd of Pd monometallic nanoclusters. Thus, Pt atoms in the core

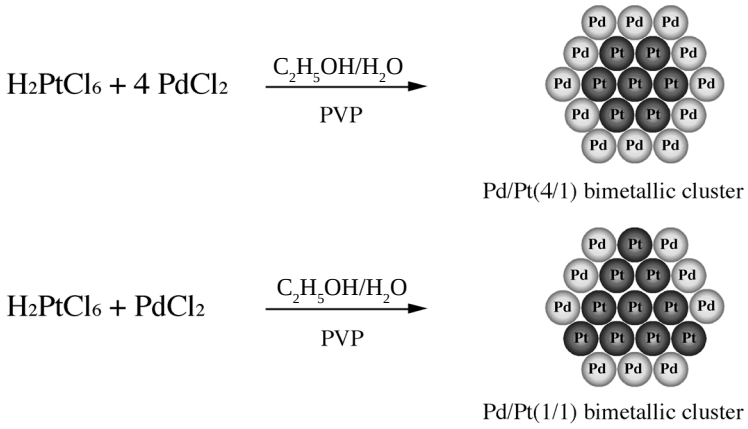

Fig. 2 Schematic illustration of formation of Pd/Pt bimetallic nanoclusters with Pd/Pt atomic ratio of 4:1 (upper) and 1:1 (lower).

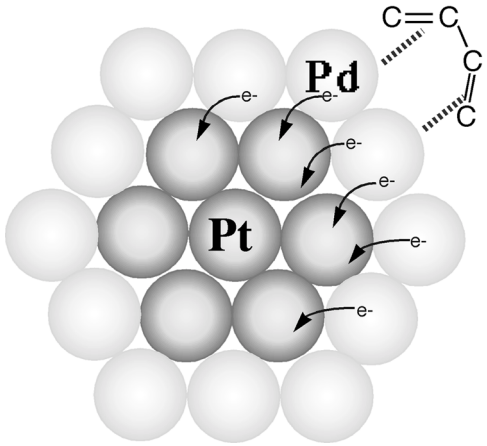

Fig. 3 Schematic illustration of the coordination of diene substrate on the surface Pd of core/shell-structured Pd/Pt bimetallic nanoclusters.

can have a strong electronic effect on the surface Pd atoms by charge transfer, resulting in rather positive Pd, which can enhance the coordination of diene as shown in Fig. 3.

The similar trends to form core/shell structures are observed for Au/Pt, Au/Pd, and Pt/Rh systems as well. The structures are analyzed by UV–vis spectra, X-ray photospectroscopy (XPS), etc., and finally confirmed by EXAFS analysis.

It is noteworthy that the core/shell structures are not always constructed when two kinds of noble metal ions are reduced simultaneously. For example, when Au and Pt ions were reduced by photoirradiation in the presence of surfactant, then not bimetallic nanoclusters, but mixtures of Au and Pt monometallic nanoclusters were obtained. Thus, both mild reduction conditions like alcohol reduction and the presence of protective polymers like PVP are very important factors to produce core/shell-structured bimetallic nanoclusters.

During the measurement in situ UV–vis spectra, fortunately we have observed the suggestion for the construction mechanism of the core/shell-structured bimetallic nanoclusters by simultaneous reduction of two kinds of noble metal ions in the presence of PVP. The construction mechanism is illustrated

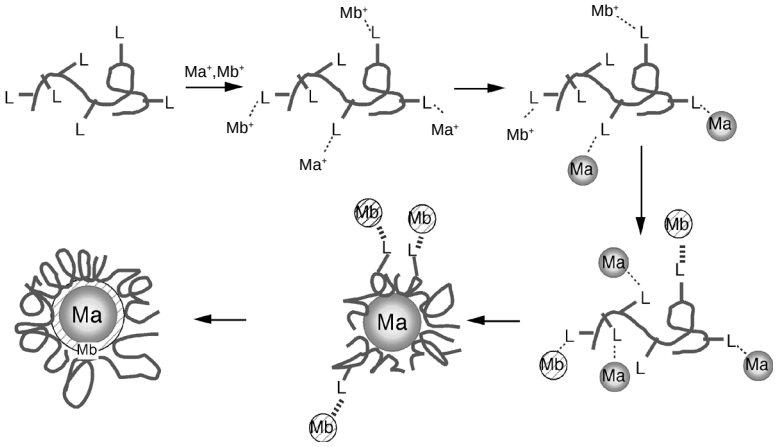

Fig. 4 Schematic illustration of the formation mechanism of core/shell-structured bimetallic nanoclusters.

in Fig. 4, where the reaction proceeds in the following processes: 1) coordination of metal ions, 2) reduction of coordinated metal ions to metal atoms or microclusters, 3) coagulation of one kind of atom or microcluster to produce core clusters, and 4) deposition of another kind of metal atom or microcluster on the surface of the core clusters to form the shells. In some cases, the step of the reduction of coordinated metal ions to metal atoms or microclusters does not occur simultaneously for two kinds of metal ions, and the early-produced metal atoms or microclusters coagulate early to form the cores. In these cases, only the order of the reduction of metal ions can control the structure. In general, however, the core/shell structures can be controlled by the following two factors: 1) reduction potential of metal ions, and 2) coordination ability of metal atoms or microclusters to the protective polymers like PVP. The latter factor can control the order of the coagulation.

VISIBLE-LIGHT-INDUCED ELECTRON TRANSFER

The colloidal dispersions of Pt nanoclusters were first applied to the catalysis for visible-light-induced hydrogen generation in an aqueous solution system like that shown in Fig. 1 because the colloidal dispersions of Pt nanoclusters are transparent and cannot disturb the light absorption by the organic dye.

As for the bimetallic nanoclusters, the colloidal dispersions of Au/Pt bimetallic nanoclusters were first reported by Harriman as the catalyst for visible-light-induced hydrogen generation in an aqueous solution [5]. In the report, Au/Pt bimetallic nanoclusters were prepared by γ-irradiation, and anything about the structure of the bimetallic nanoclusters as mentioned. We have also prepared the Au/Pt bimetallic nanoclusters by alcohol reduction in the presence of PVP. The core/shell structure has been proposed for the Au/Pt bimetallic nanoclusters as well [5]. They have higher catalytic activities for visible-light-induced hydrogen generation than the Au or Pt monometallic nanoclusters.

Under these background we have prepared various kinds of colloidal dispersions of monometallic and bimetallic nanoclusters by alcohol-reduction from the corresponding metal ions according to the following formulae.

$$2\,HAuCl_4 + 3\,C_2H_5OH \rightarrow 2\,Au + 3\,CH_3CHO + 8\,HCl \quad (1)$$

$$H_2PtCl_6 + 2\,C_2H_5OH \rightarrow Pt + 2\,CH_3CHO + 6\,HCl \quad (2)$$

$$PdCl_2 + C_2H_5OH \rightarrow Pd + CH_3CHO + 2\,HCl \quad (3)$$

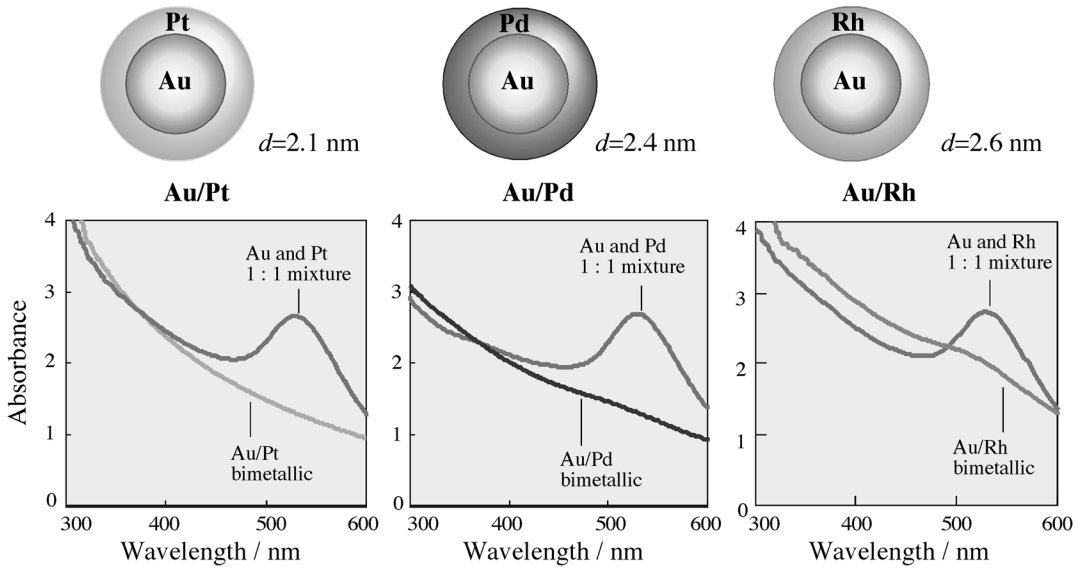

Fig. 5 Absorption spectra of colloidal dispersions of bimetallic nanoclusters and the mixtures of the corresponding monometallic nanoclusters. The core-shell structure models are also illustrated.

$$2\ RhCl_3 + 3\ C_2H_5OH \rightarrow 2\ Rh + 3\ CH_3CHO + 6\ HCl \quad (4)$$

$$2\ RuCl_3 + 3\ C_2H_5OH \rightarrow 2\ Ru + 3\ CH_3CHO + 6\ HCl \quad (5)$$

Bimetallic nanoclusters with Au-core were prepared by co-reduction of Au and Pt or Pd ions in ethanol using PVP as a protective agent. In the Au/Pt and Au/Pd bimetallic nanoclusters, the Au-core/Pt- or Pd-shell structure has been supported by UV–vis spectra, since the colloidal dispersions of bimetallic nanoclusters with an Au-core/Pt- or Pd-shell structure do not show the specific color based on the surface plasmon absorption of Au nanoclusters as shown in Fig. 5. Based on the similar consideration, the Au/Rh bimetallic nanoclusters can be proposed to have an Au-core/Rh-shell structure because the surface plasmon absorption of Au was rarely observed as shown in Fig. 5.

From TEM photographs, the particle diameter distribution histograms of Au/Pt, Au/Pd, Au/Rh, and Pt/Ru bimetallic nanoclusters were calculated as shown in Fig. 6, which indicate that the metal nanoclusters prepared here are small enough in size, ranging from 1.9 to 2.6 nm in average diameter except for Au (average diameter = 9.2 nm), and narrow in size distribution (σ = 0.8–1.6 nm).

The colloidal dispersions of monometallic and bimetallic nanoclusters thus obtained were applied as the catalysts for the visible-light-induced hydrogen generation in the system shown in Fig. 1. Hydrogen generations were measured by using GC (TCD), and increased linearly in proportion to irradiation time. The hydrogen generation rate increased with increasing concentration of colloidal metals. Some examples are shown in Fig. 7. In each case, the bimetallic nanoclusters have the higher catalytic activity than the corresponding monometallic nanoclusters. Hydrogen generation rate constant k_{H_2} of monometallic and bimetallic nanoclusters are summarized in Table 1. Among these colloidal dispersions, Pt/Ru bimetallic nanoclusters show the highest activity for the hydrogen generation.

In visible-light-induced hydrogen generation, the metal nanocluster works as an electron mediator to accept electrons from methyl viologen cation radical and donate them to protons producing hydrogen molecules. The decay rate constant of $MV^{+\cdot}$ without metal nanoclusters (k_d) was measured by tracing the fading of blue color of $MV^{+\cdot}$ using a conventional spectrophotometer, and determined to be

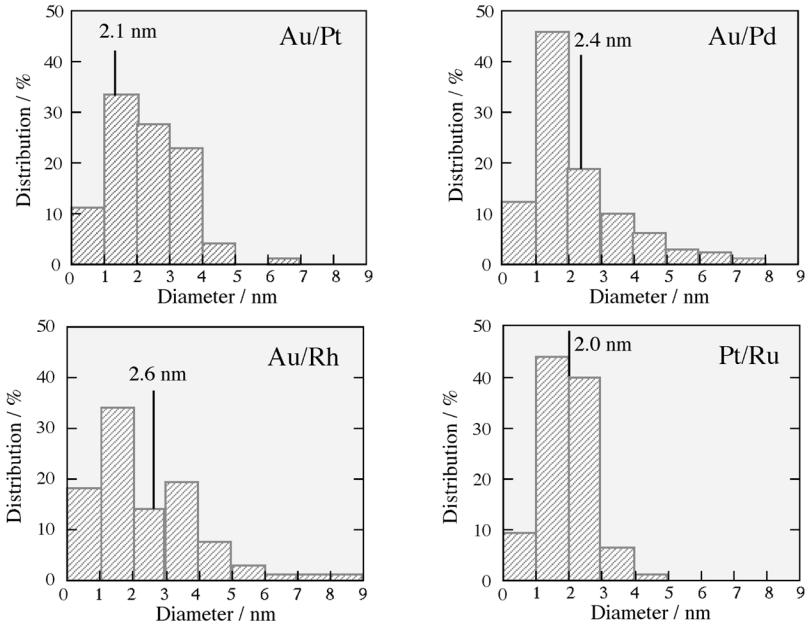

Fig. 6 Particle size distributions of Au/Pt, Au/Pd, Au/Rh, and Pt/Ru bimetallic nanoclusters.

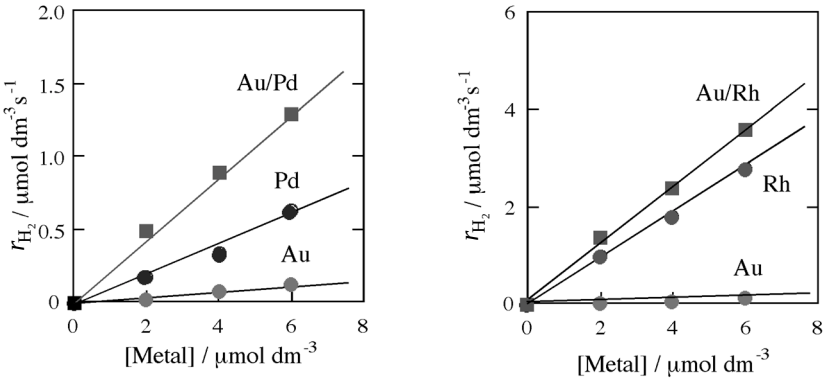

Fig. 7 The relationship between hydrogen generation rate r_{H2} and the concentration of metal in the visible-light-induced hydrogen generation in the system of Fig. 1, using Au-Pd and Au-Rh monometallic and bimetallic colloidal systems.

1.9×10^4 s^{-1} at room temperature. The decay rates of $MV^{+\cdot}$ were accelerated by addition of colloidal dispersions of metal nanoclusters to the solution because of the electron transfer from $MV^{+\cdot}$ to metal nanoclusters. The decay curve can be expressed by a single exponential way for any kind of metal nanoclusters. Thus, when k_d is a decay rate constant of $MV^{+\cdot}$ in the absence of metal nanoclusters, k_e is an electron transfer rate constant from $MV^{+\cdot}$ to metal nanocluster in the presence of metal nanoclusters, and [Metal] is the concentration of metal nanoclusters, then the decay of $MV^{+\cdot}$ can be expressed by eqs. 6 and 7. Atomic concentration, particle concentration, and total surface area of metal particles can be used for [Metal]. This selection alters the unit of k_e.

Table 1 H_2 generation rate constant k_{H2} of monometallic and bimetallic nanoclusters.

Monometallic nanocluster	$\frac{k_{H2}}{s^{-1}}$	Bimetallic nanocluster	$\frac{k_{H2}}{s^{-1}}$
Au	0.02	Au/Pd	0.23
Pd	0.10	Au/Pt	0.27
Pt	0.15	Au/Rh	0.58
Ru	0.45	Pt/Ru	0.80
Rh	0.53		

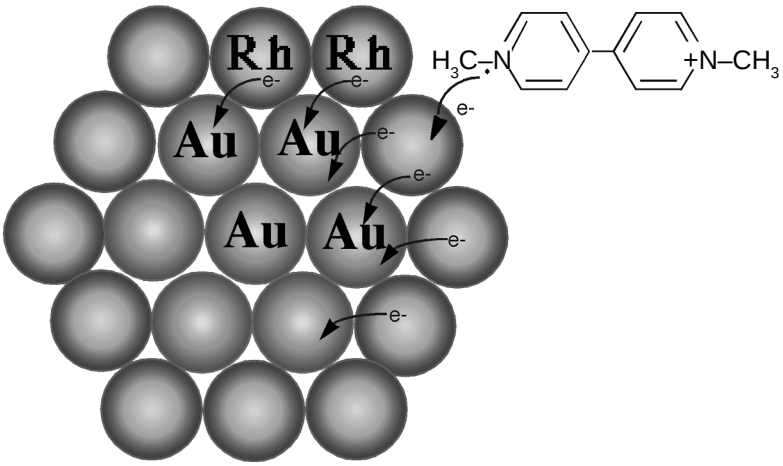

Fig. 8 Schematic illustration of electronic effect of central metal on electron transfer rate from methyl viologen cation radical to surface metal of core/shell-structured bimetallic nanoclusters.

$$-d[MV^{+\cdot}]/dt = k_{MV}[MV^{+\cdot}] \quad (6)$$

$$k_{MV} = k_d + k_e[\text{Metal}] \quad (7)$$

The constant k_e was found to depend on the kind of metal. The constant k_e of the bimetallic nanocluster is always larger than those of the corresponding monometallic nanoclusters, revealing that the bimetallic nanocluster can accept electrons more easily than the monometallic one. This can be illustrated schematically in Fig. 8. Among the bimetallic nanoclusters examined here, the Pt/Ru bimetallic nanocluster can accept electrons most easily. However, if the electron transfer rate coefficients are compared per unit surface, which can be calculated based on the average diameters, then Au/Rh bimetallic cluster is the most active.

The electron transfer rate from methyl viologen cation radical to colloidal metal particles was often thought to proceed by diffusion control. However, this is not always true. Actually, we can observe that the rate is in the order of minute by measurement of the decay rate of methyl viologen cation radical in the presence of colloidal dispersions of metal nanoclusters. This rate is much slower than the diffusion control rate. On the other hand, methyl viologen cation radical can be produced at the rate of diffusion of photosensitizer. Because the productive rate of methyl viologen cation radical is very fast,

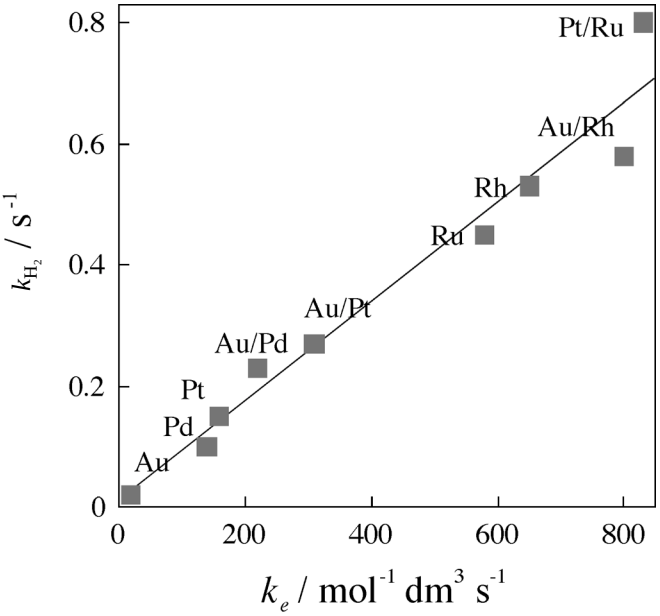

Fig. 9 Relationship between electron transfer rate constant k_e and hydrogen generation rate constant k_{H2}.

the electron transfer from methyl viologen cation radical to metal nanocluster is a rate-determining step.

The linear relationship is observed between the electron transfer rate coefficients and the hydrogen generation rate coefficient as shown in Fig. 9. This linear relationship means that the electrons, which metal nanoclusters accept from methyl viologen cation radicals, can be consumed for the hydrogen generation at a constant efficiency. This efficiency is independent of the kind of metal of nanoclusters.

CONCLUDING REMARKS

When two kinds of noble metal ions are reduced simultaneously by alcohol in the presence of PVP, the colloidal dispersions of bimetallic nanoclusters can be obtained. The bimetallic nanoclusters thus obtained often have the core/shell structure, which can be determined by UV–vis, XPS, and EXAFS analyses. The core/shell structure can be controlled by the reduction potential of metal ions and coordination ability of metal atoms or microclusters to PVP. The core/shell-structured bimetallic nanoclusters have higher catalytic activity than the corresponding monometallic nanoclusters in general. This high activity can be understood by the electronic effect of the core to the surface atoms.

The structure of various kinds of colloidal dispersions of monometallic and bimetallic nanoclusters, prepared by alcohol-reduction of noble metal ions in the presence of PVP, were analyzed by UV–vis spectra. The bimetallic nanoclusters, thus analyzed to have core/shell structures, as well as monometallic nanoclusters, work as catalysts for visible-light-induced hydrogen generation from water in the system of EDTA/$[Ru(bpy)_3]^{2+}$/MV^{2+}/metal nanocluster. The bimetallic nanoclusters are generally more active than the corresponding monometallic nanoclusters again in this case. The highest catalytic activity is observed for Au/Rh and/or Pt/Ru bimetallic nanoclusters among the metal nanoclusters examined

here. The hydrogen generation rate coefficients are in proportion to the electron transfer rate coefficient from methyl viologen cation radical to metal nanoclusters at a steady state. The higher catalytic activity of the bimetallic nanoclusters having the core/shell structure can also be understood by the electronic effect of the core upon the surface atoms.

ACKNOWLEDGMENTS

The author expresses his sincere thanks to all the coworkers who have made a great effort to achieve the good results. This work was supported by a Grant-in-Aid for Scientific Research on Priority Areas, "New Polymers and Their Nano-Organized Systems" (No. 277/08246101) from the Ministry of Education, Science, Sports, and Culture, Japan.

REFERENCES

1. H. Hirai and N. Toshima. Pages 87–140 in *Tailored Metal Catalysts* (Y. Iwasawa, D. Reidel, eds.), D. Reidel Pub., Dordrecht, 1986; G. Schmid. In *Clusters and Colloids*, VCH, Weinheim, 1994.
2. N. Toshima and T. Yonezawa. *New J. Chem*. **22**, 1179 (1998).
3. N. Toshima, M. Harada, Yonezawa, K. Kushihashi, K. Asakura. *J. Phys. Chem*. **95**, 7448 (1991); N. Toshima, M. Harada, Y. Yamazaki, K. Asakura. *J. Phys. Chem*. **96**, 9927 (1992); M. Harada, K. Asakura, N. Toshima. *J. Phys. Chem*. **98**, 2653 (1994).
4. N. Toshima, M. Kuriyama, Y. Yamada, H. Hirai. *Chem. Lett*. **1981**, 793.
5. A. Harriman. *J. Chem. Soc., Chem. Commun.* **1990**, 24; T. Yonezawa and N. Toshima. *J. Mol. Catal*. **83**, 167 (1993).
6. P. Mulvaney, M. Giersig, A. Henglein. *J. Phys. Chem*. **97**, 7061 (1993).
7. P. Mulvaney, M. Giersig, A. Henglein. *J. Phys. Chem*. **96**, 10419 (1992).
8. K. Torigoe, Y. Nakajima, K. Esumi. *J. Phys. Chem*. **97**, 8304 (1993); K. Torigoe and K. Esumi. *Langmuir* **9**, 1664 (1993).
9. H. Bönnemann, W. Brijoux, R. Brinkmann, R. Fretzen, J. Joussen, R. Köppler, B. Korall, P. Neiteler, J. Richten. *J. Mol. Catal*. **86**, 129 (1994).
10. K. Esumi, T. Tano, K. Torigoe, K. Meguro. *Chem. Mater*. **2**, 564 (1990); J. S. Bradley, E. W. Hill, C. Klein, B. Chaudret, A. Duteil. *Chem. Mater*. **5**, 254 (1993).
11. N. Toshima and Y. Wang. *Adv. Mater*. **6**, 245 (1994); N. Toshima and Y. Wang. *Chem. Lett*. **1993**, 1611; N. Toshima and Y. Wang. *Langmuir* **10**, 4574 (1994).